

## A family of range restricted iterative methods for linear discrete ill-posed problems

Laura Dykes<sup>a</sup> · Lothar Reichel<sup>a</sup>

### Abstract

The solution of large linear systems of equations with a matrix of ill-determined rank and an error-contaminated right-hand side requires the use of specially designed iterative methods in order to avoid severe error propagation. The choice of solution subspace is important for the quality of the computed approximate solution, because this solution typically is determined in a subspace of fairly small dimension. This paper presents a family of range restricted minimal residual iterative methods that modify the well-known GMRES method by allowing other initial vectors for the solution subspace. A comparison of the iterates computed by different range restricted minimal residual methods can be helpful for determining which iterates may provide accurate approximations of the desired solution. Numerical examples illustrate the competitiveness of the new methods and how iterates from different methods can be compared.

2000 AMS subject classification: 65F10, 65F22, 65N20.

Keywords: ill-posed problem, iterative method, truncated iteration.

## 1 Introduction

This paper describes a family of iterative methods for the computation of approximate solutions of linear systems of equations

$$Ax = b, \quad A \in \mathbb{R}^{m \times m}, \quad x, b \in \mathbb{R}^m, \quad (1)$$

with a large matrix  $A$  of ill-determined rank. Thus,  $A$  has many “tiny” singular values of different orders of magnitude. In particular,  $A$  is severely ill-conditioned and may be singular. Linear systems of equations (1) with a matrix of this kind are commonly referred to as linear discrete ill-posed problems. They are obtained, for instance, by the discretization of linear ill-posed problems, such as Fredholm integral equations of the first kind with a smooth kernel.

In many linear discrete ill-posed problems that arise in science and engineering, the right-hand side vector  $b$  is determined by measurement and is contaminated by an error that stems from measurement inaccuracies and possibly discretization. Thus,

$$b = \hat{b} + e, \quad (2)$$

where  $\hat{b} \in \mathbb{R}^m$  denotes the unknown error-free right-hand side. The error-vector  $e$  is referred to as “noise.”

We would like to compute the solution of minimal Euclidean norm,  $\hat{x}$ , of the linear discrete ill-posed problem with the unknown error-free right-hand side

$$Ax = \hat{b}. \quad (3)$$

Since the right-hand side is not known, we seek to determine an approximation of  $\hat{x}$  by computing an approximate solution of the available linear system of equations (1). Due to the severe ill-conditioning of the matrix  $A$  and the error  $e$  in  $b$ , the least-squares solution of minimal Euclidean norm of (1) generally does not furnish a useful approximation of  $\hat{x}$ .

A popular approach to determine a meaningful approximation of  $\hat{x}$  is to apply an iterative method to the solution of (1) and terminate the iterations sufficiently early. This type of solution approach is known as truncated iteration. One can show that the sensitivity of the computed solution to the error  $e$  increases with the number of iterations. Let  $x_k$  denote the  $k$ th iterate determined by an iterative method, such as GMRES or the conjugate gradient method applied to the normal equations  $A^T Ax = A^T b$  associated with (1). Then the difference  $x_k - \hat{x}$  typically decreases as  $k$  increases and is small, but increases with  $k$  for  $k$  large. The growth of the difference  $x_k - \hat{x}$  for large values of  $k$  is caused by severe propagation of the error  $e$  in  $b$  and of round-off errors introduced during the computations. This behavior of the iterates is commonly referred to as semiconvergence. It is important to terminate the iterations when  $x_k$  is close to  $\hat{x}$ . When an estimate of the norm of  $e$  is available, the discrepancy principle can be used to determine how many iterations to carry out. Truncated iteration based on the discrepancy principle is analyzed in, e.g., [7, 9].

<sup>a</sup>Department of Mathematical Sciences, Kent State University, Kent, OH (USA)

GMRES is a popular iterative method for the solution of large nonsymmetric linear systems that arise from the discretization of well-posed problems, such as Dirichlet boundary value problems for elliptic partial differential equations; see, e.g., Saad [19]. Let the initial iterate be  $x_0 = 0$ . Then the  $k$ th iterate,  $x_k$ , computed by GMRES applied to the solution of (1) satisfies

$$\|Ax_k - b\| = \min_{x \in \mathbb{K}_k(A, b)} \|Ax - b\|, \quad x_k \in \mathbb{K}_k(A, b), \quad (4)$$

where  $\mathbb{K}_k(A, b) = \text{span}\{b, Ab, \dots, A^{k-1}b\}$  is a Krylov subspace and  $\|\cdot\|$  denotes the Euclidean vector norm. We tacitly assume that  $k$  is sufficiently small so that  $\dim(\mathbb{K}_k(A, b)) = k$ . GMRES may determine more accurate approximations of  $\hat{x}$  with less arithmetic work than the conjugate gradient method applied to the normal equations associated with (1); see [5, 6, 8] for illustrations.

For linear discrete ill-posed problems, for which the desired solution  $\hat{x}$  is the discretization of a smooth function, it has been observed in [6, 11] that the following variant of GMRES, referred to as Range Restricted GMRES (RRGMRES), often delivers more accurate approximations of  $\hat{x}$  than GMRES. The name of the method stems from that the iterates live in  $\mathcal{R}(A)$ . Here and throughout this paper  $\mathcal{R}(M)$  denotes the range of the matrix  $M$ . Specifically, the  $k$ th iterate,  $x_k$ , determined by RRGMRRES with initial iterate  $x_0 = 0$  satisfies

$$\|Ax_k - b\| = \min_{x \in \mathbb{K}_k(A, Ab)} \|Ax - b\|, \quad x_k \in \mathbb{K}_k(A, Ab), \quad (5)$$

where  $\mathbb{K}_k(A, Ab) = \text{span}\{Ab, A^2b, \dots, A^k b\}$ . Properties of and computed examples with RRGMRRES can be found in [2, 6, 18]. A new implementation with improved numerical properties recently has been described in [13, 14].

It is the purpose of the present paper to generalize the implementation discussed in [13, 14] to be able to determine iterates  $x_k^{(\ell)}$  that solve the minimization problems

$$\|Ax_k^{(\ell)} - b\| = \min_{x \in \mathbb{K}_k(A, A^\ell b)} \|Ax - b\|, \quad x_k^{(\ell)} \in \mathbb{K}_k(A, A^\ell b), \quad \ell = 0, 1, \dots, \ell_{\max}, \quad (6)$$

for some (small) positive integer  $\ell_{\max}$ . The initial iterates  $x_0^{(\ell)}$  are defined to be the zero vector. We refer to the solution method for a particular value  $\ell$  as RRGMRRES( $\ell$ ). Thus, RRGMRRES(0) is standard GMRES (4) and RRGMRRES(1) is the method (5). RRGMRRES( $\ell$ ) is a range restricted GMRES method for  $\ell \geq 1$ .

For each RRGMRRES( $\ell$ ) method, there is (at least) one iterate  $x_{k_\ell}^{(\ell)}$  that best approximates the desired solution  $\hat{x}$ . However, it is difficult to determine which iterates are best approximations of  $\hat{x}$  unless further information about the error  $e$  or the desired solution  $\hat{x}$  is available. We propose to compute iterates for different values of  $\ell$ , say,  $x_k^{(\ell_1)}$  and  $x_k^{(\ell_2)}$  for  $\ell_1 \neq \ell_2$  and  $k = 1, 2, \dots$ , and to study the behavior of the function

$$k = k(\ell_1, \ell_2) \rightarrow \|x_k^{(\ell_1)} - x_k^{(\ell_2)}\|. \quad (7)$$

Due to the semiconvergence of the methods, we expect the iterates  $x_k^{(\ell_1)}$  and  $x_k^{(\ell_2)}$  to be close when they are accurate approximations of  $\hat{x}$ , and to differ considerably when they are severely contaminated by propagated error. Therefore, graphs of the functions (7) indicate which iterates may furnish the best approximations of  $\hat{x}$ . This information may be useful when no bound for  $\|e\|$  is available and the discrepancy principle cannot be applied to determine which iterate to choose as an approximation of  $\hat{x}$ . Information about the functions (7) may be attractive to apply in conjunction with the L-curve or generalized cross validation, two popular criteria for choosing a suitable iterate when no bound for  $\|e\|$  is known; see, e.g., [3, 4, 12, 16, 17] for discussions on several methods for determining a suitable iterate, including the L-curve and generalized cross validation. We remark that several of these references are concerned with Tikhonov regularization, an alternative to truncated iteration, but the methods discussed also can be applied to truncated iteration in slightly modified form.

This paper is organized as follows. In Section 2 we describe a solution method for the minimization problems (6) and Section 3 presents a few computed examples. Concluding remarks can be found in Section 4.

## 2 Computation of approximate solutions with RRGMRRES( $\ell$ )

We first outline the computation of the RRGMRRES(1) iterate  $x_k^{(1)}$  by the method described in [13, 14] and then discuss the computation of the iterates  $x_k^{(\ell)}$  of RRGMRRES( $\ell$ ) for  $1 < \ell \leq \ell_{\max}$ . Application of  $k$  steps of the Arnoldi process to the matrix  $A$  with initial vector  $v_1 = b/\|b\|$  gives the Arnoldi decomposition

$$AV_k = V_{k+1}H_{k+1,k}, \quad (8)$$

where  $H_{k+1,k} \in \mathbb{R}^{(k+1) \times k}$  is upper Hessenberg, the matrix  $V_{k+1} = [v_1, v_2, \dots, v_{k+1}] \in \mathbb{R}^{m \times (k+1)}$  has orthonormal columns that span the Krylov subspace  $\mathbb{K}_{k+1}(A, b)$ , and  $V_k \in \mathbb{R}^{m \times k}$  consists of the first  $k$  columns of  $V_{k+1}$ . This decomposition is the basis for the standard GMRES implementation. Its computation requires the evaluation of  $k$  matrix-vector products with the matrix  $A$ ; see Saad [19] for details.

Introduce the QR factorization

$$H_{k+1,k} = Q_{k+1}^{(1)} R_{k+1,k}^{(1)}, \quad (9)$$

where  $Q_{k+1}^{(1)} \in \mathbb{R}^{(k+1) \times (k+1)}$  is orthogonal and  $R_{k+1,k}^{(1)} \in \mathbb{R}^{(k+1) \times k}$  has a leading  $k \times k$  upper triangular submatrix,  $R_k^{(1)}$ , and a vanishing last row. Since  $H_{k+1,k}$  is upper Hessenberg, the matrix  $Q_{k+1}^{(1)}$  can be expressed as a product of  $k$  elementary reflections,

$$Q_{k+1}^{(1)} = G_1 G_2 \cdots G_k, \quad (10)$$

where  $G_j \in \mathbb{R}^{(k+1) \times (k+1)}$  is a symmetric elementary reflection in the planes  $j$  and  $j+1$ . Thus,  $G_j$  is the identity matrix except for a  $2 \times 2$  block in the rows and columns  $j$  and  $j+1$ . The representation (10) shows that  $Q_{k+1}^{(1)}$  is upper Hessenberg.

Let the matrix  $Q_{k+1,k}^{(1)} \in \mathbb{R}^{(k+1) \times k}$  consist of the first  $k$  columns of  $Q_{k+1}^{(1)}$  and introduce  $W_k^{(1)} = V_{k+1} Q_{k+1,k}^{(1)}$ . Then it follows from (8) and (9) that

$$AV_k = W_k^{(1)} R_k^{(1)}, \quad (11)$$

which shows that  $\mathcal{R}(W_k^{(1)}) = \mathbb{K}_k(A, Ab)$ . We assume for ease of exposition that all Krylov subspaces are of full dimension. Then the minimization problem (6) for  $\ell = 1$  can be written as

$$\begin{aligned} \min_{y \in \mathbb{R}^k} \|AW_k^{(1)}y - b\| &= \min_{y \in \mathbb{R}^k} \|AV_{k+1}Q_{k+1,k}^{(1)}y - b\| \\ &= \min_{y \in \mathbb{R}^k} \|V_{k+2}H_{k+2,k+1}Q_{k+1,k}^{(1)}y - b\| \\ &= \min_{y \in \mathbb{R}^k} \|H_{k+2,k+1}Q_{k+1,k}^{(1)}y - e_1\| \|b\|, \end{aligned}$$

where  $e_1 = [1, 0, \dots, 0]^T$  denotes the first axis vector and the last equality follows from the fact that  $V_{k+2}e_1 = b/\|b\|$ . The matrices  $V_{k+2}$  and  $H_{k+2,k+1}$  are obtained by applying  $k+1$  steps of the Arnoldi process to the matrix  $A$  with initial vector  $v_1 = b/\|b\|$ . Thus, they are determined by the decomposition (8) with  $k$  replaced by  $k+1$ .

Since both matrices  $H_{k+2,k+1}$  and  $Q_{k+1,k}^{(1)}$  are upper Hessenberg, their product vanishes below the sub-subdiagonal. It follows that the QR factorization

$$H_{k+2,k+1}Q_{k+1,k}^{(1)} = Q_{k+2}^{(2)}R_{k+2,k}^{(2)}$$

can be computed in only  $\mathcal{O}(k^2)$  arithmetic floating point operations with the aid of elementary reflections. Here  $Q_{k+2}^{(2)} \in \mathbb{R}^{(k+2) \times (k+2)}$  is orthogonal with zero entries below the sub-subdiagonal and  $R_{k+2,k}^{(2)} \in \mathbb{R}^{(k+2) \times k}$  has a leading  $k \times k$  upper triangular submatrix,  $R_k^{(2)}$ , and two vanishing last rows. Thus,

$$AW_k^{(1)} = V_{k+2}Q_{k+2}^{(2)}R_{k+2,k}^{(2)} \quad (12)$$

and

$$\min_{y \in \mathbb{R}^k} \|AW_k^{(1)}y - b\| = \min_{y \in \mathbb{R}^k} \|R_{k+2,k}^{(2)}y - (Q_{k+2}^{(2)})^T e_1\| \|b\|. \quad (13)$$

Let  $y_k^{(1)}$  denote the solution of (13). Then the solution of RRGMR(1) is given by  $x_k^{(1)} = W_k^{(1)}y_k^{(1)}$ .

The solution of RRGMR(2) can be computed analogously. Thus, let  $W_k^{(2)}$  consist of the first  $k$  columns of the matrix  $V_{k+2}Q_{k+2}^{(2)}$ . The relation

$$AW_k^{(1)} = W_k^{(2)}R_k^{(2)}$$

follows from (12) and shows that  $\mathcal{R}(W_k^{(2)}) = \mathbb{K}(A, A^2b)$ . The minimization problem for RRGMR(2) can be expressed as

$$\begin{aligned} \min_{y \in \mathbb{R}^k} \|AW_k^{(2)}y - b\| &= \min_{y \in \mathbb{R}^k} \|AV_{k+2}Q_{k+2,k}^{(2)}y - b\| \\ &= \min_{y \in \mathbb{R}^k} \|V_{k+3}H_{k+3,k+2}Q_{k+2,k}^{(2)}y - b\| \\ &= \min_{y \in \mathbb{R}^k} \|H_{k+3,k+2}Q_{k+2,k}^{(2)}y - e_1\| \|b\|, \end{aligned}$$

where the matrices  $V_{k+3}$  and  $H_{k+3,k+2}$  are determined by applying  $k+2$  steps of the Arnoldi process to the matrix  $A$  with initial vector  $v_1 = b/\|b\|$ , and the matrix  $Q_{k+2,k}^{(2)} \in \mathbb{R}^{(k+2) \times k}$  is obtained by removing the last two columns from  $Q_{k+2}^{(2)}$ .

Consider the QR factorization

$$H_{k+3,k+2}Q_{k+2,k}^{(2)} = Q_{k+3}^{(3)}R_{k+3,k}^{(3)}, \quad (14)$$

where  $Q_{k+3}^{(3)} \in \mathbb{R}^{(k+3) \times (k+3)}$  is orthogonal and  $R_{k+3,k}^{(3)} \in \mathbb{R}^{(k+3) \times k}$  has a leading  $k \times k$  upper triangular submatrix and three vanishing last rows. Due to the structure of  $H_{k+3,k+2}$  and  $Q_{k+2,k}^{(2)}$ , the matrix  $Q_{k+3}^{(3)}$  vanishes below the sub-sub-subdiagonal. Therefore, the factorization (14) can be computed in only  $\mathcal{O}(k^2)$  arithmetic floating point operations by the application of a judicious choice of elementary reflections.

We obtain analogously to (13) that

$$\min_{y \in \mathbb{R}^k} \|AW_k^{(2)}y - b\| = \min_{y \in \mathbb{R}^k} \|R_{k+3,k}^{(3)}y - (Q_{k+3}^{(3)})^T e_1\| \|b\|.$$

Denote the solution by  $y_k^{(2)}$ . The  $k$ th iterate of RRGMR(2) then is given by  $x_k^{(2)} = W_k^{(2)}y_k^{(2)}$ .

We may proceed in this manner to determine matrices  $W_k^{(\ell)} \in \mathbb{R}^{m \times k}$  such that  $\mathcal{R}(W_k^{(\ell)}) = \mathbb{K}(A, A^\ell b)$  and compute solutions  $x_k^{(\ell)}$  of the RRGMR( $\ell$ ) minimization problem for  $\ell = 3, 4, \dots, \ell_{\max}$ . The computation of these solutions requires the evaluation of  $k + \ell_{\max}$  matrix-vector products with the matrix  $A$ . These matrix-vector product evaluations constitute the dominating computational work for large-scale problems. Typically, only few iterations have to be carried out. This is illustrated in the following section.

### 3 Computed examples

We apply RRGMRES( $\ell$ ) methods to the solution of several standard test problems to illustrate the performance of these methods. All computations are carried out in MATLAB with about 15 significant decimal digits.

Example 3.1. Let the matrix  $A$  be obtained by discretizing the integral equation of the first kind

$$\int_{-\pi/2}^{\pi/2} \kappa(\tau, \sigma)x(\sigma)d\sigma = b(\tau), \quad -\frac{\pi}{2} \leq \tau \leq \frac{\pi}{2}, \tag{15}$$

where

$$\kappa(\sigma, \tau) = (\cos(\sigma) + \cos(\tau)) \left( \frac{\sin(\xi)}{\xi} \right)^2, \quad \xi = \pi(\sin(\sigma) + \sin(\tau)).$$

The right-hand side function  $b(\tau)$  is chosen so that the solution  $x(\sigma)$  is the sum of two Gaussian functions. This integral equation is discussed by Shaw [20]. We discretize it by a Nyström method based on the composite trapezoidal rule with  $n = 1000$  equidistant nodes. This yields the nonsymmetric matrix  $A \in \mathbb{R}^{1000 \times 1000}$  and the discretized solution  $\hat{x} \in \mathbb{R}^{1000}$  from which we determine  $\hat{b} = A\hat{x}$ . A vector  $e \in \mathbb{R}^{1000}$  with normally distributed random entries with zero mean simulates noise; it is scaled to correspond to a specified noise-level

$$v = \frac{\|e\|}{\|\hat{b}\|}. \tag{16}$$

We determine the contaminated right-hand side in (1) from (2). In our initial computations, we let  $v = 0.01$ .

iterative method	error for best iterate
RRGMRES(0)	$\ x_6^{(0)} - \hat{x}\  = 4.30$
RRGMRES(1)	$\ x_5^{(1)} - \hat{x}\  = 4.01$
RRGMRES(2)	$\ x_7^{(2)} - \hat{x}\  = 2.06$
RRGMRES(3)	$\ x_7^{(3)} - \hat{x}\  = 2.06$
RRGMRES(4)	$\ x_7^{(4)} - \hat{x}\  = 2.05$

Table 1: Example 3.1: Best iterates generated by RRGMRES( $\ell$ ) for  $\ell = 0, 1, \dots, 4$ , and smallest errors achieved for noise-level  $v = 0.01$ .

Table 1 displays the smallest differences  $\|x_k^{(\ell)} - \hat{x}\|$  achieved with RRGMRES( $\ell$ ) for  $0 \leq \ell \leq 4$ . The quality of the best approximation of  $\hat{x}$  is seen to increase as  $\ell$  grows from 0 to 4. The table suggests that when the desired solution  $\hat{x}$  is the discretization of a smooth function, then it may be beneficial to use RRGMRES( $\ell$ ) with  $\ell \geq 2$ .

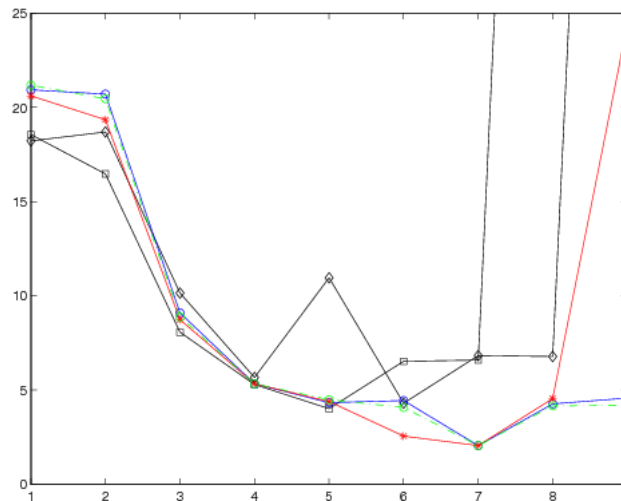
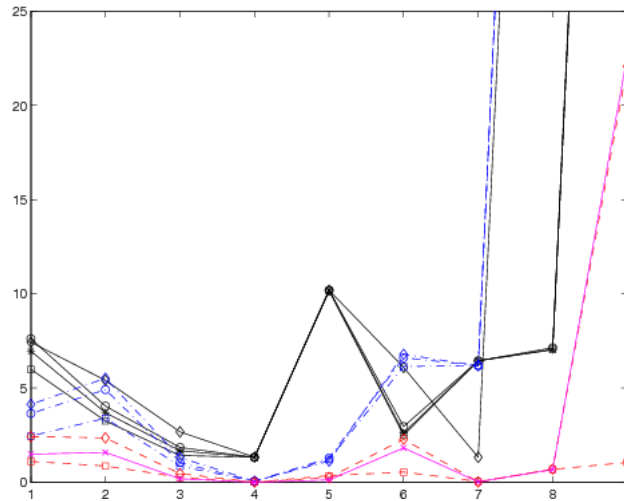


Figure 1: Example 3.1: Errors in approximate solutions  $x_k^{(\ell)}$  for  $0 \leq \ell \leq 4$  and  $1 \leq k \leq 9$ . The (black) diamonds connected by solid lines show  $\|x_k^{(0)} - \hat{x}\|$ , the (black) squares connected by solid lines depict  $\|x_k^{(1)} - \hat{x}\|$ , the (blue) circles connected by solid lines display  $\|x_k^{(2)} - \hat{x}\|$ , the (red) stars connected by solid lines show  $\|x_k^{(3)} - \hat{x}\|$ , and the (green) circles connected by dash-dotted lines depict  $\|x_k^{(4)} - \hat{x}\|$ . The noise-level is  $v = 0.01$ .

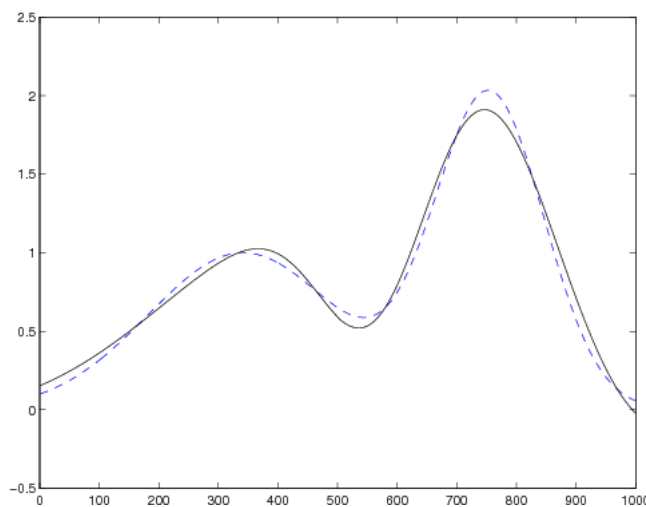
Figure 1 displays the errors  $\|x_k^{(\ell)} - \hat{x}\|$  for  $0 \leq \ell \leq 4$  and  $1 \leq k \leq 9$ . The RRGMRES( $\ell$ ) methods for  $\ell = 2, 3, 4$  are seen to determine iterates with the smallest errors at step 7.

Figure 2 shows differences in norm between pairs of iterates  $x_k^{(\ell_1)}$  and  $x_k^{(\ell_2)}$  for  $1 \leq k \leq 9$  and  $\ell_1 \neq \ell_2$ . The (black) solid graphs marked by diamonds, squares, circles, and stars show the differences between the RRGMRES(0) iterates and iterates



**Figure 2:** Example 3.1: Differences in iterates  $\|x_k^{(\ell_1)} - x_k^{(\ell_2)}\|$  for  $0 \leq \ell_1 \neq \ell_2 \leq 4$  and  $1 \leq k \leq 9$ . The (black) diamonds connected by solid lines show  $\|x_k^{(0)} - x_k^{(1)}\|$ , the (black) squares connected by solid lines depict  $\|x_k^{(0)} - x_k^{(2)}\|$ , the (black) circles connected by solid lines display  $\|x_k^{(0)} - x_k^{(3)}\|$ , the (black) stars connected by solid lines display  $\|x_k^{(0)} - x_k^{(4)}\|$ , the (blue) diamonds connected by dash-dotted lines show  $\|x_k^{(1)} - x_k^{(2)}\|$ , the (blue) squares connected by dash-dotted lines depict  $\|x_k^{(1)} - x_k^{(3)}\|$ , the (blue) circles connected by solid lines display  $\|x_k^{(1)} - x_k^{(4)}\|$ , the (red) diamonds connected by dashed lines show  $\|x_k^{(2)} - x_k^{(3)}\|$ , the (red) squares connected by dashed lines depict  $\|x_k^{(2)} - x_k^{(4)}\|$ , and the (magenta) “x” connected by solid lines display  $\|x_k^{(3)} - x_k^{(4)}\|$ . The noise-level is  $\nu = 0.01$ .

generated by  $\text{RRGMRES}(\ell)$  for  $\ell \geq 1$ . These graphs can be found at the top of the figure, which indicates that the iterates computed by  $\text{RRGMRES}(0)$  differ significantly from many of the iterates determined by  $\text{RRGMRES}(\ell)$  for  $\ell \geq 1$ . The (blue) dash-dotted graphs marked by diamonds, squares, and circles display the difference between iterates generated by  $\text{RRGMRES}(1)$  and those computed by  $\text{RRGMRES}(\ell)$  for  $\ell \geq 2$ . All the (blue) graphs are fairly close together and quite near the top of the figure, except for  $k = 4$ . This suggests that the  $\text{RRGMRES}(1)$  iterates, for  $k \neq 4$ , differ significantly from the approximate solutions computed by  $\text{RRGMRES}(\ell)$  for  $\ell > 1$ . The (red) dashed graphs marked with diamonds and squares display how much the iterates  $x_k^{(2)}$  differ from  $x_k^{(3)}$  and  $x_k^{(4)}$ , respectively. These graphs are close to the bottom of the figure, and so is the (magenta) solid graph marked with x, which displays how much the  $\text{RRGMRES}(3)$  and  $\text{RRGMRES}(4)$  iterates differ. Figure 2 suggests that the iterates  $x_k^{(\ell)}$  for  $\ell \geq 1$  and  $x_7^{(\ell)}$  for  $\ell \geq 2$  may be accurate approximations of  $\hat{x}$ . The latter of these iterates might furnish the most accurate approximations of  $\hat{x}$  since they have had a chance to pick up more information about the matrix  $A$  than the iterates  $x_4^{(\ell)}$  and have not diverged away from each other. Table 1 shows that, indeed, the iterates  $x_7^{(\ell)}$  for  $\ell \geq 2$  provide the most accurate approximations of  $\hat{x}$ . Figure 3 depicts the vectors  $\hat{x}$  and  $x_7^{(4)}$ .



**Figure 3:** Example 3.1: Computed approximate solution  $x_7^{(4)}$  (black) solid curve and desired solution  $\hat{x}$  (blue) dashed curve. The noise-level is  $\nu = 0.01$ .

The above computations illustrate that it may be advantageous to let  $\ell \geq 2$  in  $\text{RRGMRES}(\ell)$  when the noise-level (16) is 0.01.

	$\nu = 1 \cdot 10^{-3}$	$\nu = 1 \cdot 10^{-4}$
iterative method	error for best iterate	error for best iterate
RRGMRES(0)	$\ x_7^{(0)} - \hat{x}\  = 1.77$	$\ x_8^{(0)} - \hat{x}\  = 1.63$
RRGMRES(1)	$\ x_7^{(1)} - \hat{x}\  = 1.76$	$\ x_7^{(1)} - \hat{x}\  = 1.64$
RRGMRES(2)	$\ x_7^{(2)} - \hat{x}\  = 1.65$	$\ x_8^{(2)} - \hat{x}\  = 1.50$
RRGMRES(3)	$\ x_7^{(3)} - \hat{x}\  = 1.65$	$\ x_{10}^{(3)} - \hat{x}\  = 1.49$
RRGMRES(4)	$\ x_7^{(4)} - \hat{x}\  = 1.65$	$\ x_9^{(4)} - \hat{x}\  = 1.48$

**Table 2:** Example 3.1: Best iterates generated by RRGMRES( $\ell$ ) for  $\ell = 0, 1, \dots, 4$ , and smallest errors achieved for two noise-levels.

Table 2 shows that this may be the case also for smaller noise-levels.  $\square$

Example 3.2. The matrix of this example is obtained by discretizing the integral equation of the first kind

$$\int_{-6}^6 \kappa(t,s)x(s)ds = b(t), \quad -6 \leq t \leq 6, \tag{17}$$

discussed by Phillips [15]. Its solution, kernel, and right-hand side are given by

$$\begin{aligned} x(s) &= \begin{cases} 1 + \cos(\frac{\pi}{3}s), & \text{if } |s| < 3, \\ 0, & \text{otherwise,} \end{cases} \\ \kappa(t,s) &= x(t-s), \\ b(t) &= (6 - |t|)(1 + \frac{1}{2} \cos(\frac{\pi}{3}t)) + \frac{9}{2\pi} \sin(\frac{\pi}{3}|t|). \end{aligned}$$

We discretize this integral equation by a Nyström method based on a composite trapezoidal quadrature rule with 1000 equidistant nodes. This gives the nonsymmetric matrix  $A \in \mathbb{R}^{1000 \times 1000}$ . A discretization of the exact solution defines  $\hat{x} \in \mathbb{R}^{1000}$  and we let  $\hat{b} = A\hat{x}$ . The contaminated right-hand side  $b \in \mathbb{R}^{1000}$  is defined analogously as in Example 3.1. The noise-level is  $\nu = 0.01$  unless specified otherwise.

iterative method	error for best iterate
RRGMRES(0)	$\ x_{10}^{(0)} - \hat{x}\  = 0.782$
RRGMRES(1)	$\ x_8^{(1)} - \hat{x}\  = 0.550$
RRGMRES(2)	$\ x_9^{(2)} - \hat{x}\  = 0.466$
RRGMRES(3)	$\ x_9^{(3)} - \hat{x}\  = 0.504$
RRGMRES(4)	$\ x_9^{(4)} - \hat{x}\  = 0.458$

**Table 3:** Example 3.2: Best iterates generated by RRGMRES( $\ell$ ) for  $\ell = 0, 1, \dots, 4$ , and smallest errors achieved. The noise-level is  $\nu = 0.01$ .

Table 3 is analogous to Table 1 and displays the smallest differences  $\|x_k^{(\ell)} - \hat{x}\|$  achieved with RRGMRES( $\ell$ ) for  $0 \leq \ell \leq 4$ . Similarly as for Table 1, the present table shows that letting  $\ell \geq 2$  may improve the accuracy of the best iterate  $x_k^{(\ell)}$ .

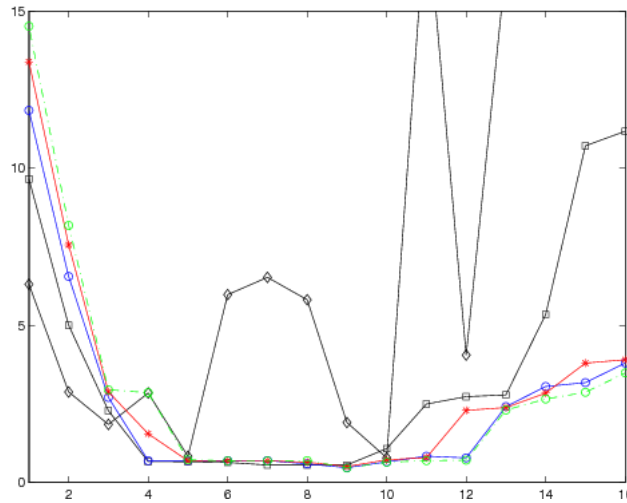
Figure 4 displays the errors  $\|x_k^{(\ell)} - \hat{x}\|$  for  $0 \leq \ell \leq 4$  and  $1 \leq k \leq 16$ , and shows the iterates  $x_k^{(\ell)}$  determined by RRGMRES( $\ell$ ) for  $\ell \geq 2$  to be accurate approximations of  $\hat{x}$  for  $5 \leq k \leq 9$ .

Figure 5 shows differences in norm between pairs of iterates  $x_k^{(\ell_1)}$  and  $x_k^{(\ell_2)}$  for  $1 \leq k \leq 16$  and  $0 \leq \ell_1 \neq \ell_2 \leq 4$ . This figure is analogous to Figure 2. The closeness of the red and magenta graphs for  $6 \leq k \leq 10$  indicates that the iterates  $x_k^{(\ell)}$  for these values of  $k$  and  $3 \leq \ell \leq 4$  furnish accurate approximations of  $\hat{x}$ . This is in agreement with Figure 4. Figure 6 shows the vectors  $\hat{x}$  and  $x_9^{(4)}$ .

	$\nu = 1 \cdot 10^{-3}$	$\nu = 1 \cdot 10^{-4}$
iterative method	error for best iterate	error for best iterate
RRGMRES(0)	$\ x_8^{(0)} - \hat{x}\  = 0.284$	$\ x_{12}^{(0)} - \hat{x}\  = 0.099$
RRGMRES(1)	$\ x_{10}^{(1)} - \hat{x}\  = 0.176$	$\ x_{14}^{(1)} - \hat{x}\  = 0.072$
RRGMRES(2)	$\ x_{12}^{(2)} - \hat{x}\  = 0.176$	$\ x_{17}^{(2)} - \hat{x}\  = 0.063$
RRGMRES(3)	$\ x_{11}^{(3)} - \hat{x}\  = 0.215$	$\ x_{17}^{(3)} - \hat{x}\  = 0.066$
RRGMRES(4)	$\ x_{12}^{(4)} - \hat{x}\  = 0.176$	$\ x_{18}^{(4)} - \hat{x}\  = 0.061$

**Table 4:** Example 3.2: Best iterates generated by RRGMRES( $\ell$ ) for  $\ell = 0, 1, \dots, 4$ , and smallest errors achieved for two noise-levels.

Table 3 shows that it may be beneficial to let  $\ell \geq 2$  in RRGMRES( $\ell$ ) when the noise-level (16) is 0.01. Table 4 indicates that this also is true for smaller noise-levels.  $\square$



**Figure 4:** Example 3.2: Errors in approximate solutions  $x_k^{(\ell)}$  for  $0 \leq \ell \leq 4$  and  $1 \leq k \leq 16$ . The (black) diamonds connected by solid lines show  $\|x_k^{(0)} - \hat{x}\|$ , the (black) squares connected by solid lines depict  $\|x_k^{(1)} - \hat{x}\|$ , the (blue) circles connected by solid lines display  $\|x_k^{(2)} - \hat{x}\|$ , the (red) stars connected by solid lines show  $\|x_k^{(3)} - \hat{x}\|$ , and the (green) circles connected by dash-dotted lines depict  $\|x_k^{(4)} - \hat{x}\|$ . The noise-level is  $\nu = 0.01$ .

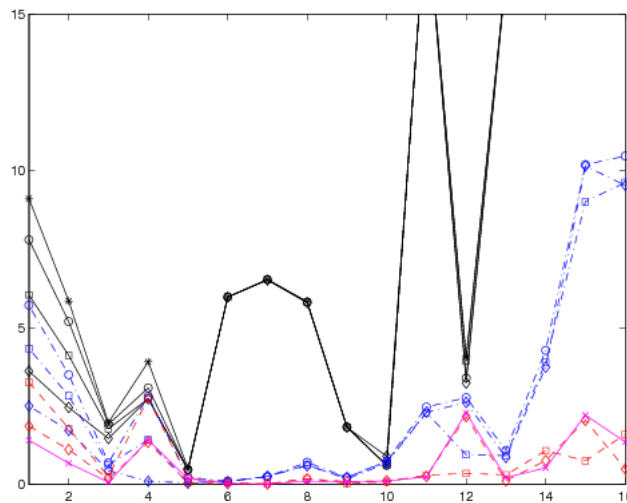


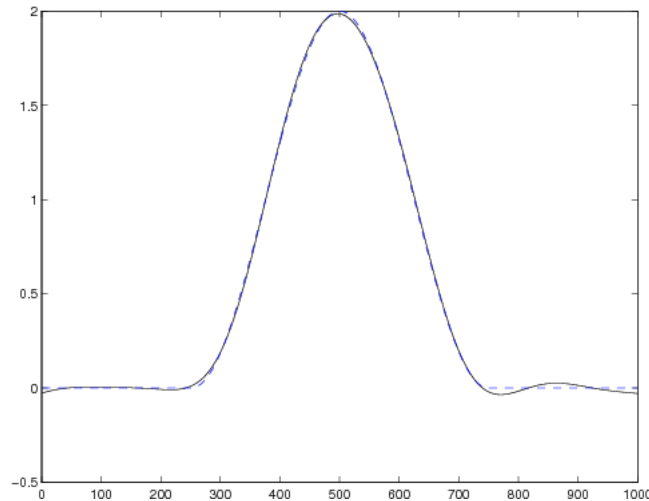
**Figure 5:** Example 3.2: Differences in iterates  $\|x_k^{(\ell_1)} - x_k^{(\ell_2)}\|$  for  $0 \leq \ell_1 \neq \ell_2 \leq 4$  and  $1 \leq k \leq 16$ . The (black) diamonds connected by solid lines show  $\|x_k^{(0)} - x_k^{(1)}\|$ , the (black) squares connected by solid lines depict  $\|x_k^{(0)} - x_k^{(2)}\|$ , the (black) circles connected by solid lines display  $\|x_k^{(0)} - x_k^{(3)}\|$ , the (black) stars connected by solid lines display  $\|x_k^{(0)} - x_k^{(4)}\|$ , the (blue) diamonds connected by dash-dotted lines show  $\|x_k^{(1)} - x_k^{(2)}\|$ , the (blue) squares connected by dash-dotted lines depict  $\|x_k^{(1)} - x_k^{(3)}\|$ , the (blue) circles connected by solid lines display  $\|x_k^{(1)} - x_k^{(4)}\|$ , the (red) diamonds connected by dashed lines show  $\|x_k^{(2)} - x_k^{(3)}\|$ , the (red) squares connected by dashed lines depict  $\|x_k^{(2)} - x_k^{(4)}\|$ , and the (magenta) “x” connected by solid lines display  $\|x_k^{(3)} - x_k^{(4)}\|$ . The noise-level is  $\nu = 0.01$ .

Example 3.3. The Fredholm integral equation of the first kind

$$\int_0^\pi \kappa(\sigma, \tau)x(\tau)d\tau = b(\sigma), \quad 0 \leq \sigma \leq \frac{\pi}{2}, \tag{18}$$

with  $\kappa(\sigma, \tau) = \exp(\sigma \cos(\tau))$ ,  $b(\sigma) = 2 \sinh(\sigma)/\sigma$ , and solution  $x(\tau) = \sin(\tau)$  is discussed by Baart [1]. We use the MATLAB code baart from [10] to discretize (18) by a Galerkin method with 1000 orthonormal box functions as test and trial functions. The code produces the nonsymmetric matrix  $A \in \mathbb{R}^{1000 \times 1000}$  and the scaled discrete approximation  $\hat{x} \in \mathbb{R}^{1000}$  of  $x(\tau)$ . The noise-free right-hand side is given by  $\hat{b} = A\hat{x}$ . The entries of the noise vector  $e \in \mathbb{R}^{1000}$  are generated in the same way as in Example 3.1. Unless specified otherwise, the noise-level is  $\nu = 1 \cdot 10^{-3}$ . The contaminated right-hand side is defined by (2).

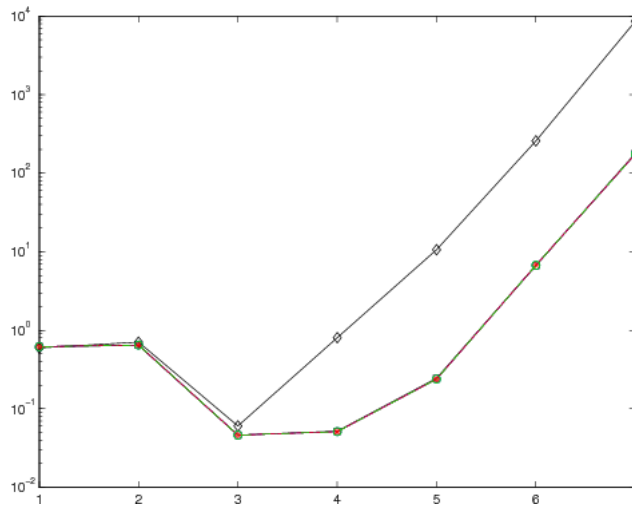
Table 5 shows the smallest differences  $\|x_k^{(\ell)} - \hat{x}\|$  achieved by RGMRES( $\ell$ ) for  $0 \leq \ell \leq 4$ . For this example the RGMRES( $\ell$ ) methods for  $\ell \geq 1$  perform about the same, and better than RGMRES(0). In particular, the table illustrates that letting  $\ell \geq 2$  does not result in worse approximations of  $\hat{x}$  than  $\ell = 1$ .



**Figure 6:** Example 3.2: Computed approximate solution  $x_9^{(4)}$  (black) solid curve and desired solution  $\hat{x}$  (blue) dashed curve. The noise-level is  $\nu = 0.01$ .

iterative method	error for best iterate
RRGMRES(0)	$\ x_3^{(0)} - \hat{x}\  = 0.058$
RRGMRES(1)	$\ x_3^{(1)} - \hat{x}\  = 0.045$
RRGMRES(2)	$\ x_3^{(2)} - \hat{x}\  = 0.045$
RRGMRES(3)	$\ x_3^{(3)} - \hat{x}\  = 0.045$
RRGMRES(4)	$\ x_3^{(4)} - \hat{x}\  = 0.045$

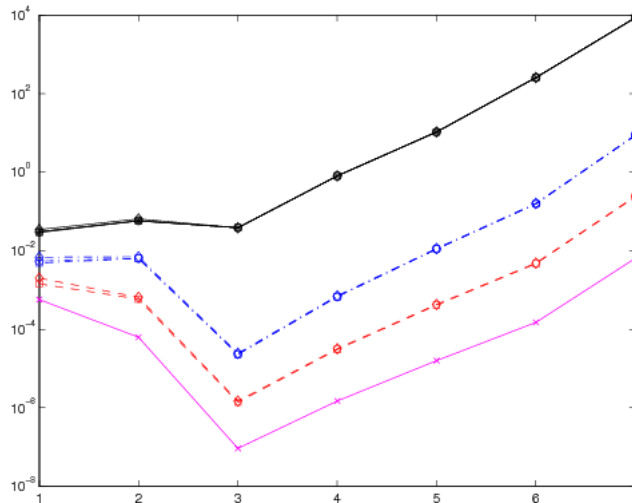
**Table 5:** Example 3.3: Best iterates generated by RRGMRRES( $\ell$ ) for  $\ell = 0, 1, \dots, 4$ , and smallest errors achieved. The noise-level is  $\nu = 1 \cdot 10^{-3}$ .



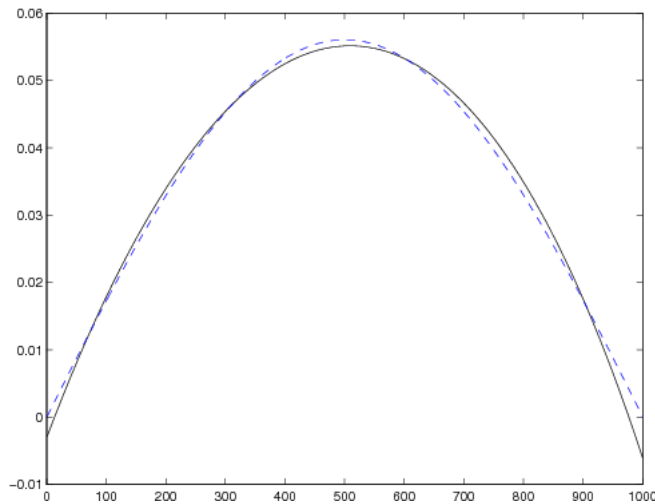
**Figure 7:** Example 3.3: Errors in approximate solutions  $x_k^{(\ell)}$  for  $0 \leq \ell \leq 4$  and  $1 \leq k \leq 7$ . The (black) diamonds connected by solid lines show  $\|x_k^{(0)} - \hat{x}\|$ , the (black) squares connected by solid lines depict  $\|x_k^{(1)} - \hat{x}\|$ , the (blue) circles connected by solid lines display  $\|x_k^{(2)} - \hat{x}\|$ , the (red) stars connected by solid lines show  $\|x_k^{(3)} - \hat{x}\|$ , and the (green) circles connected by dash-dotted lines depict  $\|x_k^{(4)} - \hat{x}\|$ . The noise-level is  $\nu = 1 \cdot 10^{-3}$ .

Figure 7 is analogous to Figure 4, but with a logarithmic scale for the vertical axis. The figure shows all RRGMRRES( $\ell$ ) methods for  $\ell \geq 1$  to perform about the same, and the best iterate determined by RRGMRRES(0) is seen to differ more from  $\hat{x}$  than the iterates computed by the other methods. This is in agreement with Table 5.

Figure 8 is similar to Figure 5, but uses a logarithmic scale for the vertical axis. The figure shows the iterates  $x_3^{(3)}$  and  $x_3^{(4)}$  to be very close. This suggests that these iterates may be accurate approximations of  $\hat{x}$ , which is in agreement with Table 5. Figure 9 displays  $x_3^{(4)}$  and  $\hat{x}$ . Finally, Table 6 illustrates that it may be beneficial to let  $\ell \geq 2$  in RRGMRRES( $\ell$ ) also for noise-levels different



**Figure 8:** Example 3.3: Differences in iterates  $\|x_k^{(\ell_1)} - x_k^{(\ell_2)}\|$  for  $0 \leq \ell_1 \neq \ell_2 \leq 4$  and  $1 \leq k \leq 7$ . The (black) diamonds connected by solid lines show  $\|x_k^{(0)} - x_k^{(1)}\|$ , the (black) squares connected by solid lines depict  $\|x_k^{(0)} - x_k^{(2)}\|$ , the (black) circles connected by solid lines display  $\|x_k^{(0)} - x_k^{(3)}\|$ , the (black) stars connected by solid lines display  $\|x_k^{(0)} - x_k^{(4)}\|$ , the (blue) diamonds connected by dash-dotted lines show  $\|x_k^{(1)} - x_k^{(2)}\|$ , the (blue) squares connected by dash-dotted lines depict  $\|x_k^{(1)} - x_k^{(3)}\|$ , the (blue) circles connected by solid lines display  $\|x_k^{(1)} - x_k^{(4)}\|$ , the (red) diamonds connected by dashed lines show  $\|x_k^{(2)} - x_k^{(3)}\|$ , the (red) squares connected by dashed lines depict  $\|x_k^{(2)} - x_k^{(4)}\|$ , and the (magenta) “x” connected by solid lines display  $\|x_k^{(3)} - x_k^{(4)}\|$ . The noise-level is  $\nu = 1 \cdot 10^{-3}$ .



**Figure 9:** Example 3.3: Computed approximate solution  $x_3^{(4)}$  (black) solid curve and desired solution  $\hat{x}$  (blue) dashed curve. The noise-level is  $\nu = 1 \cdot 10^{-3}$ .

iterative method	$\nu = 1 \cdot 10^{-2}$	$\nu = 1 \cdot 10^{-4}$
	error for best iterate	error for best iterate
RRGMRES(0)	$\ x_3^{(0)} - \hat{x}\  = 0.393$	$\ x_3^{(0)} - \hat{x}\  = 0.045$
RRGMRES(1)	$\ x_3^{(1)} - \hat{x}\  = 0.069$	$\ x_5^{(1)} - \hat{x}\  = 0.024$
RRGMRES(2)	$\ x_3^{(2)} - \hat{x}\  = 0.068$	$\ x_5^{(2)} - \hat{x}\  = 0.023$
RRGMRES(3)	$\ x_3^{(3)} - \hat{x}\  = 0.068$	$\ x_5^{(3)} - \hat{x}\  = 0.023$
RRGMRES(4)	$\ x_4^{(4)} - \hat{x}\  = 0.068$	$\ x_5^{(4)} - \hat{x}\  = 0.023$

**Table 6:** Example 3.3: Best iterates generated by RRGMRRES( $\ell$ ) for  $\ell = 0, 1, \dots, 4$ , and smallest errors achieved for two noise-levels.

from  $1 \cdot 10^{-3}$ . □

## 4 Conclusion

This paper describes new range restricted GMRES methods. The examples shown, as well as numerous other computed examples, indicate that RRGMRRES( $\ell$ ) for  $\ell \geq 2$  can give iterates that approximate the desired solution  $\hat{x}$  better than iterates determined by RRGMRRES( $\ell$ ) for  $\ell \leq 1$ . Moreover, computation of the norm of differences of iterates determined by different RRGMRRES( $\ell$ ) methods may yield useful information about which iterates provide the most accurate approximations of  $\hat{x}$ .

## Acknowledgements

The second author's research has been supported in part by NSF grant DMS-1115385. The authors would like to thank a referee for useful comments.

## References

- [1] M. L. Baart, The use of auto-correlation for pseudo-rank determination in noisy ill-conditioned least-squares problems, *IMA J. Numer. Anal.*, 2 (1982), pp. 241–247.
- [2] J. Baglama and L. Reichel, Augmented GMRES-type methods, *Numer. Linear Algebra Appl.*, 14 (2007), pp. 337–350.
- [3] C. Brezinski, M. Redivo-Zaglia, G. Rodriguez, and S. Seatzu, Multi-parameter regularization techniques for ill-conditioned linear systems, *Numer. Math.*, 94 (2003), pp. 203–228.
- [4] C. Brezinski, G. Rodriguez, and S. Seatzu, Error estimates for linear systems with applications to regularization, *Numer. Algorithms*, 49 (2008), pp. 85–104.
- [5] D. Calvetti, B. Lewis, and L. Reichel, Restoration of images with spatially variant blur by the GMRES method, in *Advanced Signal Processing Algorithms, Architectures, and Implementations X*, ed. F. T. Luk, Proceedings of the Society of Photo-Optical Instrumentation Engineers (SPIE), vol. 4116, The International Society for Optical Engineering, Bellingham, WA, 2000, pp. 364–374.
- [6] D. Calvetti, B. Lewis, and L. Reichel, On the choice of subspace for iterative methods for linear discrete ill-posed problems, *Int. J. Appl. Math. Comput. Sci.*, 11 (2001), pp. 1069–1092.
- [7] D. Calvetti, B. Lewis, and L. Reichel, On the regularizing properties of the GMRES method, *Numer. Math.*, 91 (2002), pp. 605–625.
- [8] D. Calvetti, B. Lewis, and L. Reichel, GMRES, L-curves, and discrete ill-posed problems, *BIT*, 42 (2002), pp. 44–65.
- [9] H. W. Engl, M. Hanke, and A. Neubauer, *Regularization of Inverse Problems*, Kluwer, Dordrecht, 1996.
- [10] P. C. Hansen, Regularization tools version 4.0 for Matlab 7.3, *Numer. Algorithms*, 46 (2007), pp. 189–194.
- [11] P. C. Hansen and T. K. Jensen, Noise propagation in regularizing iterations for image deblurring, *Electron. Trans. Numer. Anal.*, 31 (2008), pp. 204–220.
- [12] S. Kindermann, Convergence analysis of minimization-based noise level-free parameter choice rules for linear ill-posed problems, *Electron. Trans. Numer. Anal.*, 38 (2011), pp. 233–257.
- [13] A. Neuman, L. Reichel, and H. Sadok, Implementations of range restricted iterative methods for linear discrete ill-posed problems, *Linear Algebra Appl.*, 436 (2012), pp. 3974–3990.
- [14] A. Neuman, L. Reichel, and H. Sadok, Algorithms for range restricted iterative methods for linear discrete ill-posed problems, *Numer. Algorithms*, 59 (2012), pp. 325–331.
- [15] D. L. Phillips, A technique for the numerical solution of certain integral equations of the first kind, *J. ACM*, 9 (1962), pp. 84–97.
- [16] L. Reichel and G. Rodriguez, Old and new parameter choice rules for discrete ill-posed problems, *Numer. Algorithms*, 63 (2013), pp. 65–87.
- [17] L. Reichel, G. Rodriguez, and S. Seatzu, Error estimates for large-scale ill-posed problems, *Numer. Algorithms*, 51 (2009), pp. 341–361.
- [18] L. Reichel and Q. Ye, Breakdown-free GMRES for singular systems, *SIAM J. Matrix Anal. Appl.*, 26 (2005), pp. 1001–1021.
- [19] Y. Saad, *Iterative Methods for Sparse Linear Systems*, 2nd ed., SIAM, Philadelphia, 2003.
- [20] C. B. Shaw, Jr., Improvements of the resolution of an instrument by numerical solution of an integral equation, *J. Math. Anal. Appl.*, 37 (1972), pp. 83–112.